G-quadruplex based biosensor: A potential tool for SARS-CoV-2 detection

Hui Xi [a], Mario Juhas [b], Yang Zhang [a,*]

[a] College of Science, Harbin Institute of Technology (Shenzhen), Shenzhen, Guangdong, 518055, China
[b] Medical and Molecular Microbiology Unit, Department of Medicine, Faculty of Science and Medicine, University of Fribourg, Fribourg, Switzerland

ARTICLE INFO

Keywords:
G-quadruplex
Biosensor
Electrochemical biosensor
Optical biosensor
Virus detection
SARS-CoV-2

ABSTRACT

G-quadruplex is a non-canonical nucleic acid structure formed by the folding of guanine rich DNA or RNA. The conformation and function of G-quadruplex are determined by a number of factors, including the number and polarity of nucleotide strands, the type of cations and the binding targets. Recent studies led to the discovery of additional advantageous attributes of G-quadruplex with the potential to be used in novel biosensors, such as improved ligand binding and unique folding properties. G-quadruplex based biosensor can detect various substances, such as metal ions, organic macromolecules, proteins and nucleic acids with improved affinity and specificity compared to standard biosensors. The recently developed G-quadruplex based biosensors include electrochemical and optical biosensors. A novel G-quadruplex based biosensors also show better performance and broader applications in the detection of a wide spectrum of pathogens, including SARS-CoV-2, the causative agent of COVID-19 disease. This review highlights the latest developments in the field of G-quadruplex based biosensors, with particular focus on the G-quadruplex sequences and recent applications and the potential of G-quadruplex based biosensors in SARS-CoV-2 detection.

1. Introduction

G-quadruplex nucleic acid structure differs from the typical double helix. G-quadruplex is a stable coplanar tetragonal secondary structure of nucleic acids formed by the pairing of four guanine bases via Hoogsteen hydrogen bond. The interaction of four guanines forms a guanine quartet structure, which serves as the structural unit and building block for G-quadruplex structure (Dai et al., 2007; Johnson et al., 2008). G-quadruplex structure has multiple conformations, which can be formed by stacking of two, three or more G-quartets (Raguseo et al., 2020). G-quadruplexes are normally composed of four Gn ($n \geq 2$) tracts. According to the strand direction, the G-quadruplex structure can be parallel, anti-parallel and mixed (hybrid of parallel and antiparallel). The conformation of G-quadruplex is affected by many factors, including the number and polarity of nucleotide strands, the type of cations and the binding targets (Lou et al., 2014; Liu et al., 2019). G-quadruplex has several advantages due to its unique structure with increased thermodynamic and chemical stability. Because G-quadruplex structure has twice the negative charge density of double stranded DNA, it can improve its electrostatic interaction with positively charged binding ligands.

Furthermore, various G-quadruplex nucleic acids have been developed to inhibit the proliferation of tumors or to treat diseases (Tateishi-Karimata et al., 2018). G-quadruplex has many unique properties in ligands binding (Yuan et al., 2020). For example, G-quadruplex DNA under some physiological conditions resembles enzyme catalysis. In the presence of alkali metal ions, guanine rich DNA sequence can fold to a G-quadruplex structure and form a DNAzyme with catalytic activity through π - π interaction with the metalloporphyrin ring (Wang et al., 2017). The porphyrin compound N-methylporphyrin dipropionate IX (NMM) can specifically combine with G-quadruplex to produce strong fluorescence, while the triplet, dimer and single chain do not have this property. It has been reported that the combination of NMM and G-quadruplex can detect metal ions (Liu et al., 2011). G-quadruplex is widely used in biosensors to detect organic molecules (Viglasky and Hianik, 2013), nucleic acids (Tang et al., 2012), biological enzymes (Wang et al., 2015b)and metal ions (Guo et al., 2012). In recent years, G-quadruplex based biosensors have been intensively studied. Their main advantages include low detection limit and price, simple operation, fast detection ability and high sensitivity (Gao et al., 2012).

Coronavirus Disease 2019 (COVID-19, previously called 2019-nCoV) is a new infectious disease of human beings (Yu et al., 2020). The International Committee on Taxonomy of viruses has named the causative agent of COVID-19, Severe acute respiratory syndrome coronavirus 2

* Corresponding author.
E-mail addresses: zhangyang07@hit.edu.cn, yang.zhang2020@hotmail.com (Y. Zhang).

(SARS-CoV-2) (Zou et al., 2020). COVID-19 disease caused by SARS-CoV-2 is spreading rapidly all over the world and has been declared a global health emergency. Patients infected with SARS-CoV-2 show a wide range of symptoms, including cough, fever, headache, chest tightness and other acute symptoms, or may even die of disease. Asymptomatic or mild cases have also been reported (Wang et al., 2020; Chen et al., 2020). At present, there is no specific vaccine or drug to treat or prevent SARS-CoV-2 infection. Therefore, early diagnosis or detection of SARS-CoV-2 is very important for the prevention and control of the pandemic. Although, several commercial SARS-CoV-2 detection methods have been developed recently, point-of-care testing (POCT) devices are still urgently needed as a result of increasing healthcare pressures for faster turnaround of testing results. It is therefore crucial to develop novel, sensitive biosensors for rapid and specific SARS-CoV-2 detection. G-quadruplex has been shown to inhibit and detect a wide variety of viruses, including severe acute respiratory syndrome coronavirus (SARS-CoV) (Tan et al., 2009), human immunodeficiency virus (HIV) (Liang et al., 2011), and hepatitis A virus (HAV) (Ma et al., 2017). The G-quadruplex based biosensor is therefore a promising potential tool for SARS-CoV-2 detection.

In this review, we introduce the formation of G-quadruplex structure, and the design and application of G-quadruplex based biosensors. We discuss the current research progress in the development of G-quadruplex biosensors and their potential application in SARS-CoV-2 detection.

2. The structure of G-quadruplex

As a guanine (G) rich sequence, G-quadruplex forms a square plane to arrange four guanine bases (Fig. 1). The guanine bases in each plane interact via the Hoogsteen hydrogen bond (Gao et al., 2012). Sequences with the potential to form G-quadruplex have been found in different organisms' genomes (Gatto et al., 2009).

G-quadruplex can be formed from one, two or four separate strands of DNA (or RNA) with G-rich sequence. Then, the topological structure of G-quadruplexes can be classified into unimolecular, bimolecular and tetramolecular. In general, the intramolecular (unimolecular) G-quadruplex is predicted to form with the sequence of $G_{(\geq 2)}N_xG_{(\geq 2)}N_yG_{(\geq 2)}N_zG_{(\geq 2)}$. N_x, N_y and N_z can be any combination of nucleotides, including G, forming the loops. x, y and z might be different. A loop usually has one to seven nucleotides (Raguseo et al., 2020). The arrangement and combination of loop sequences affect the stability of folded G-quadruplex (Gibriel and Adel, 2017). Two layers are just about sufficient to form a G-quadruplex (Gao et al., 2012). G-quadruplex with two G-tetrads generally exhibit lower stability compared to the one with at least three or more G-tetrads. Unimolecular G-quadruplex with two layers of G-tetrads contains $GGN_XGGN_XGGN_XGG$ sequences (Fig. 2A). The most well-known is AS1411 with GGTGGTGGTGGTTGTGGTGGTGGTGG sequence (Perrone et al., 2016). The unimolecular G-quadruplex with three G-tetrads is formed by $GGGN_XGGGN_XGGGN_XGGG$ sequences. For example, cancer detection G-quadruplex (T40214) targeting STAT3 is GGGCGGGCGGGCGGGC (Fig. 2B) (Yuan et al., 2020). The unimolecular G-quadruplex can also be formed with more than three G-tetrads (Fig. 2C). Different from unimolecular, bimolecular G-quadruplex is formed by the association of two identical sequences $N_xG_{(\geq 2)}N_yG_{(\geq 2)}N_z$, where x and z may or may not be zero. Tetramolecular G-quadruplex may be formed by four $N_xG_{(\geq 2)}N_y$ or $G_{(\geq 2)}N_xG_{(\geq 2)}$ strands associating together (Gao et al., 2012; Burge et al., 2006).

G-quadruplex structure itself also has a variety of conformations, including antiparallel, parallel and hybrid (Fig. 3). Parallel G-quadruplex is formed by four strands oriented in the same direction (Fig. 3A, D). Because of the 2′- hydroxy group of ribose in pentose phosphate skeleton, RNA G-quadruplex is more inclined to form a stable, parallel G-quadruplex (Murat and Balasubramanian, 2014). G-quadruplex is described as antiparallel when at least one of the four strands is antiparallel to the others. This type of topology is found in many unimolecular and the majority of bimolecular structures (Fig. 3B, E) (Phillips et al., 1997).

The formation of the structure depends on the intermediate monovalent cations, such as K^+ and Na^+ (Cheng et al., 2017). The valence cation enters the middle of two adjacent G-quadruplex structures and combines with eight hydroxyl oxygen atoms of nucleotide. It can neutralize the negative electrostatic potential produced by oxygen atoms in eight guanines. Due to the free energy and radius of cation, G-quadruplex combines more likely with K^+. The results show that divalent cations also promote the formation of G-quadruplex, but the mechanism is more complex. The stability order of G-quadruplex and divalent cations is $Sr^{2+} > Ba^{2+} > Ca^{2+} > Mg^{2+}$ (Smargiasso et al., 2008). In addition, the ion concentration also affects the stability of G-quadruplex. The transition metal complexes binding with numerous G-quadruplex configurations can also be used to quantitatively detect metal ions (Liu et al., 2011).

In addition to metal ions, temperature, pH and reactive oxygen species (ROS) also affect the stability of G-quadruplex (Viglasky and Hianik, 2013). Temperature affects the thermodynamic stability, folding and unfolding kinetics of G-quadruplex. The effect of temperature on the stability of the folded structure of G-quadruplex is usually investigated by thermal induced unfolding experiments. Melting temperature (T_m), a characteristic parameter of G-quadruplex unfolding process, is usually 15–90 °C (Olsen and Marky, 2009; Gargallo, 2014). G-quadruplex with a specific loop can undergo conformational transition when pH changes, which is caused by the rearrangement of bonding modes (Yan et al., 2013). When pH is lower than 3.5, the G-quadruplex structure is completely destroyed, which is due to the destruction of Hoogsteen key by H^+. When pH is higher than 12, cations are not conducive to the stability and maintenance of G-quadruplex structure, and G-quadruplex conformation is also destroyed (Zhou and Yuan, 2007). In the

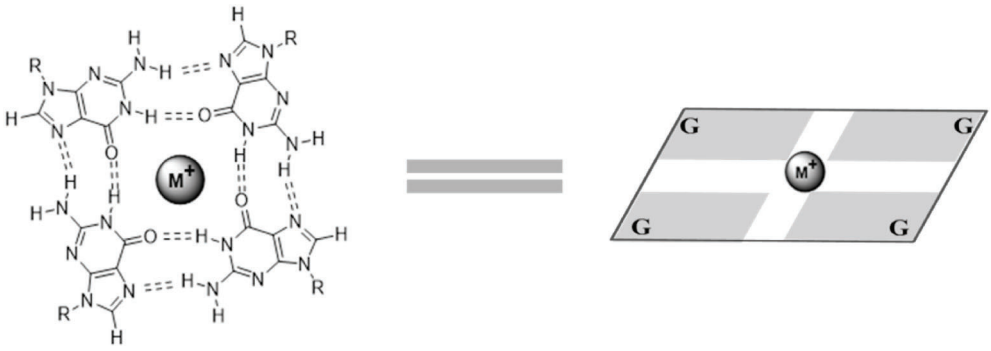

Fig. 1. The structure of G-quadruplex. The G-quartet, the structural unit of the G-quadruplex, is a square plane formed by connecting four guanines through eight hydrogen bonds. The monovalent cations are in the middle of the G square (Yuan et al., 2020).

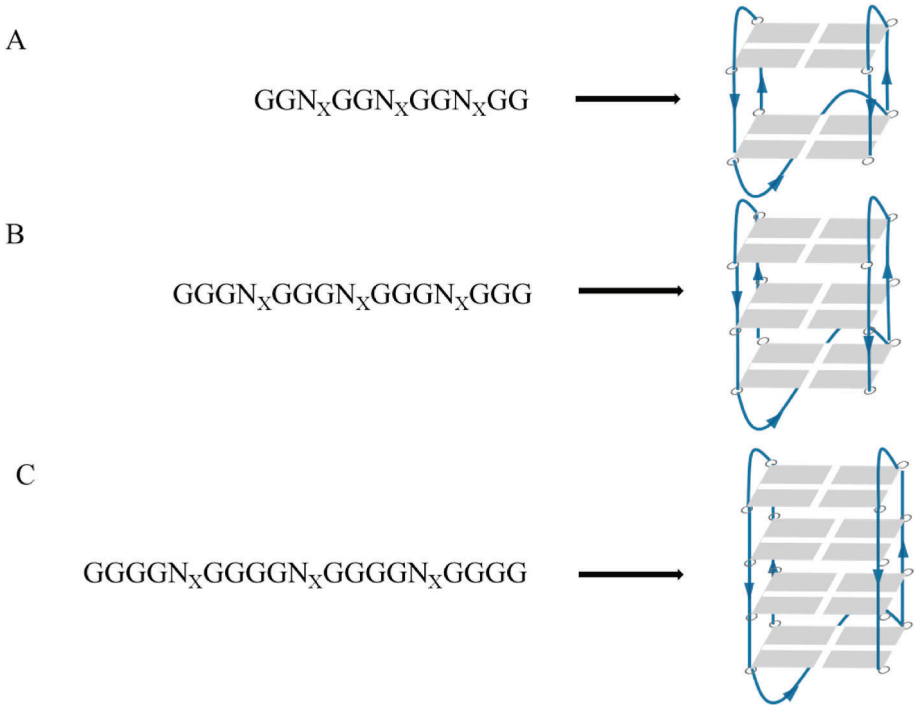

Fig. 2. Structure diagram of unimolecular G-quadruplex with two (A), three (B) and four (C) layers of G-tetrads. The loops are highlighted blue. (N_x: N denotes any of A, G, C, T, or U; $1 < x < 7$). (For interpretation of the references to color in this figure legend, the reader is referred to the Web version of this article.)

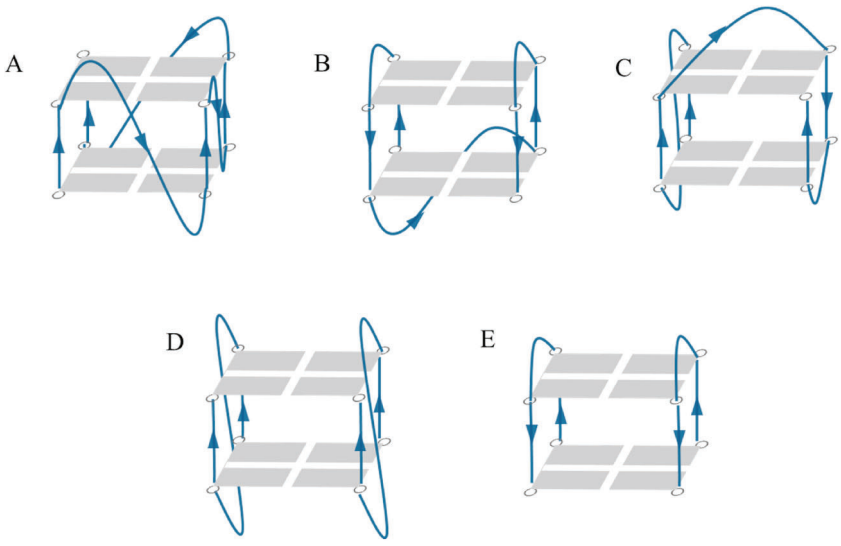

Fig. 3. The loop of G-quadruplexes. The loops are highlighted blue. The unimolecular G-quadruplex conformations include parallel (A), antiparallel (B) and hybrid (C). The bimolecular G-quadruplex conformations include parallel (D) and antiparallel (E). (For interpretation of the references to color in this figure legend, the reader is referred to the Web version of this article.)

appropriate pH range, G-quadruplex is relatively stable under acidic conditions. pH not only affects the formation of G-quadruplex, but also the binding selectivity of G-quadruplex (Tuntiwechapikul et al., 2006). ROS are a byproduct of aerobic cell metabolism leading to irreversible DNA damage. Oxidative stress causes various types of DNA damage, including strand breaks and base modifications (Bielskutė et al., 2019). Guanine bases in the G-quadruplex are sensitive to oxidative damage. A loss of G-quadruplex structure was observed for most oligonucleotides with oxidative damage (Fedeles, 2017). Notably, G-quadruplex structures are more stable in a wider range of temperature and pH than antibodies.

The G-quadruplex sequences are present in promoters, genomes, untranslated regions and the ends of chromosomes (telomeres). As a result of their locations, G-quadruplex is considered to play essential biological roles. To directly visualization and monitoring of G-quadruplex structures in live cells, several *in vivo* G-quadruplex detection methods were developed. Small molecules are able to bind and stabilize the G-quadruplex structures (Biffi et al., 2013). Thus, a number of small molecules have been used as probes for tracking the dynamic of G-quadruplex *in vivo*. Shivalingam et al. (2015) designed a small fluorescent molecule used as an optical probe for G-quadruplexes. Combing with fluorescence lifetime optical microscopy, this new probe was used to monitor G-quadruplex in living cells. Zhang et al. (2018b) reported a novel fluorescent probe, IMT, for real-time detecting DNA G-quadruplex

structure in living cells. Di Antonio et al. (2020) reported a G-quadruplex specific fluorescent probe (SiR-PyPDS) for single-molecule and real-time detection of G-quadruplex in living cells, without perturbing the formation and kinetics of G-quadruplex. In addition, visualization and detection of the dynamic folding and unfolding of RNA G-quadruplex in living cells have also attracted great interest (Laguerre et al., 2015; Chen et al., 2018).

G-quadruplex nucleic acid can be screened by Systematic Evolution of Ligands by Exponential Enrichment (SELEX) *in vitro* (Zhang et al., 2019b). Once G-quadruplex DNA structures have been formed, their thermodynamic properties are more stable than that of double stranded DNA. Moreover, the unfolding kinetics of G-quadruplex is much slower than that of DNA or RNA hairpin structures. G-quadruplex structure may hinder DNA and RNA metabolism and formation (Tauchi et al., 2006; Gowan, 2002; Rhodes and Lipps, 2015).

3. G-quadruplex based biosensor

G-quadruplex can inhibit transcription, translation and DNA replication, and act as a carrier of nanoparticles (Johnson et al., 2008). In addition, by converting binding event into detectable signals, G-quadruplex can be used as a probe in the biosensor to detect metal ions, proteins and nucleic acids. Moreover, in the presence of oxygen, G-quadruplex structure has the peroxidase activity, which can catalyze for instance 2,2-diazo-bis (3-ethyl-benzothiazole-6-sulfonic acid) diammonium salt (ABTS) (Li et al., 2012).

G-quadruplex based biosensor is composed of two parts: one is the recognition element, i.e. the G-quadruplex nucleic acid (DNA or RNA probe) which is used to recognize the target for the test; the other is the converter, which can convert the biological binding activity into the electrical, optical or vibration frequency signals for observation (Pelossof et al., 2011). G-quadruplex probe displayed highly selective reaction for different G-quadruplex DNA sequences over single stranded DNA (ssDNA), double stranded DNA (dsDNA) and triplex forming oligonucleotides (TFO) (Wang et al., 2015a). TFO bind in the major groove of dsDNA with high specificity and affinity (Frank-Kamenetskii and Mirkin, 1995; Kuauert, 2001). As a result, TFO structure can inhibit the binding of sequence specific DNA binding proteins and transcription factors, thus interfering with DNA replication and transcription. The TFO bind to the purine-rich chain of the DNA double strand via Hoogsteen hydrogen bonds. Because of these characteristics, TFO can be used as a diagnostic tool to identify foreign DNA or disease-related mutations (Fujii et al., 2019). However, the detection range of G-quadruplex is much wider. In the presence of some targets, the binding capacity of G-quadruplex is stronger than that of ssDNA, dsDNA and TFO. Bhattacharjee et al. (2016) reported that the interaction of fisetin to G-quadruplex DNA is more preferential than dsDNA. The complementary C-rich chains of G-quadruplex can adopt the i-motif structure held together by intercalated $C{\cdot}C^{+}$ pairs (Peng et al., 2009). I-motif is a four-strands DNA structure, which can form in the sequences rich in cytosine with regulatory functions (Zeraati et al., 2018). Under the near physiological conditions of pH, temperature and salt concentration, DNA mainly forms double-helix structure. However, G-quadruplex and i-motif are more easily formed at lower pH or at higher temperatures (Phan, 2002). G-quadruplex based biosensors have attracted more research interest than those based on i-motif quadruplex DNA. The detection can be realized by the signal change before and after the G-quadruplex binding to the target molecule (Liu et al., 2017). DNA sensors modified to detect metal ions such as Hg^{2+} were reported. Nucleic acid-based biosensors are widely used in molecular diagnosis (Liu et al., 2017), pathology (Cagnin et al., 2009), toxicology (Chen et al., 2016), and molecular sequencing (Yuan et al., 2018). Among those, G-quadruplex based biosensor has also been used for analysis and detection of different targets recently (Table 1).

Table 1
G-quadruplex based biosensor for analysis and detection of different targets.

Target	Sequence	Detection method	Limit of Detection	Linear detection range	Ref.
Hg^{2+}	5′-HS-$(CH_2)_6$-TTTGGGTAGGGCGGGTTGGG-3′	Surface plasmon resonance	20 nmol/L	20–200 nmol/L	Pelossof et al. (2011)
Pb^{2+}	5′-TCATGGGTGGGTGGGTGGGTGA-NH_2–3′	Electrochemistry	3.6×10^{-14} mol/L	1×10^{-13}–5×10^{-11} mol/L	Deng et al. (2016)
Cu^{2+}	–	Electrochemistry	60 fM	0.1pM–5.0 nM	Xu et al. (2015)
cholesterol	5′-GTGGGTAGGGCGGGTTGG-3′	Colorimetry	1–30 μmol/L	0.10 μmol/L	Li et al. (2012)
HBV	5′–HS–$(CH_2)_6$–TTTCCCTACCCTTGGTGGGCGTTCACGGTGGTCTCTTTGGGTAGGGCGGGTTGGG-3′	Electrochemistry	0.5 pM	10 pM-10 nM	Shi et al. (2015)
S1 nuclease	5′-GGGAAAGGGAAAGGGAAAGGG-3′	Colorimetry	5.2×10^{-2} U/mL	1×10^{-1}–1 U/mL	Wang et al. (2015a)
thrombin	5′-GGTTGGTGTGGTTGG-3′	Colorimetry	15 fM	0.05 pM–60 nM	Chen et al. (2016)
H_2O_2	5′-GGTGGTGGTGGTTGTGGTGGTGGTGG-3′	Electrochemistry	2.2 mmol/L	0.01–1.5 mmol/L	Gao et al. (2012)
lysozyme	5′-CGTATCGTATGTTCGTTGGGTAGGGCGGGTTGGG-3′	Fluorescence	2.6 nM	5.0–500 nM	Qiu et al. (2017)
prostate specific antigen	5′–SH–TTAATCCTCAGCTTATTGGGTAGGGCGGGTTGGGATGTT-3′	Photoelectrochemistry	1.8 pg/mL	0.005–50 ng/mL	Zhang et al. (2018)
alpha-fetoprotein	5′–SH–CTTAACCCGGGTGGGGAGGGTGGGCCCAA-3′	Photoelectrochemistry	14.7 pg/mL	50 pg/mL–20 ng/mL	Lv et al. (2017)
alkaline phosphatase	5′-GGGTAGGGCGGGTTGGGCTTTAAAAAAAAAAAAA-3′	Electrochemistry	0.03 U/L	0.1–5 U/L	Liu et al. (2017)

3.1. Electrochemical G-quadruplex biosensor

3.1.1. Electrochemical G-quadruplex DNA biosensor

G-quadruplex is widely used in electrochemical DNA biosensors. Compared to the standard DNA biosensor, the label-free electrochemical DNA biosensor does not require labelling of the electroactive substance on the nucleic acid probe (Zhang et al., 2018a). G-quadruplex acts as a label-free probe molecule in electrochemical DNA biosensor. Compared with common biosensors, the advantages of G-quadruplex based biosensors include high affinity, stability and sensitivity, flexibility in design, low cost and easy regeneration (Zhang et al., 2018b). G-rich ssDNA can fold into G-quadruplex structure under certain ionic strength (Wu et al., 2017). G-quadruplex structures can specifically interact with different target molecules and are therefore used to detect metal ions (Debnath et al., 2020), protein (Margulies and Hamilton, 2009), biomolecules (Wang et al., 2015b), enzymes (Nie et al., 2015) and others.

G-quadruplex is a very stable square plane arrangement of four guanine bases whose formation depends on the intermediate cations (Liu et al., 2020). Pb^{2+} as a common heavy metal ion and non-degradable environmental pollutant is a common target of biosensors. Pb^{2+} can bind to guanine rich nucleic acid, which folds to form strong specific coordination of G-quadruplex. An electrochemical sensor based on G-quadruplex DNA/Pb^{2+} structure for highly sensitive Pb^{2+} detection was constructed recently (Li et al., 2012). First, cyclodextrin and gold electrode were self-assembled, then hairpin like G-rich ssDNA was modified to the electrode, which can specifically recognize Pb^{2+}. The interaction of ssDNA and Pb^{2+} forms G-quadruplex/Pb^{2+} structure used for quantitative detection of Pb^{2+} through the change of electrical signal intensity. The sensor improves the signal-to-noise ratio and sensitivity. The presence of metal ions leading to structural changes of nucleic acid (Fig. 4). The formation of G-quadruplex structure for improved sensitivity of the sensor was also successfully used for the detection of other metal ions, such as Sr^{2+}, Hg^{2+} and Cu^{2+} with detection limit as low as nM level (Pelossof et al., 2011; Kong et al., 2010a; Huang et al., 2019). Xu et al. (2015) designed a DNA enzyme binding agent based on heme/G-tetramer, which was used as an in-situ amplification impedance sensor coupled with copper (II) ion and DNA enzyme. The relative standard deviation (RSD) was 8.5% and 9.1% for the same and different batches of sensors, respectively. The electrochemical biosensors are easy to use and do not need to be labeled, which is convenient for large-scale applications (Liu et al., 2017).

Studies have shown that G-quadruplex and hemin form a complex, which can be used as a signal alone or as a horseradish peroxidase (HRP) to catalyze the reduction of H_2O_2 and generate electrochemical signals (Ge et al., 2014). G-rich nucleic acids form G-quadruplex chains with the participation of metal ions and hemin. G-rich nucleic acids can induce the modified heme to form a G-quadruplex structure, which leads to self-assembly of heme and G-quadruplex structure. If the target detector is endonuclease, G-quadruplex structure is destroyed and the signal is changed to achieve detection (Wang et al., 2015b). Huang et al. (2019) studied a sensitive electrochemical detection method of gastric cancer exosomes based on hemin/G-quadruplex signal amplification strategy. Liu et al. (2017) reported that EAD2 (G-quadruplex structure) can also bind to Methylene blue (MB), and its binding ability is higher than ssDNA and dsDNA. This is because the structure of G-quadruplex makes it more difficult for the negatively charged $[Fe(CN)_6]^{3-/4-}$ to approach the electrode surface than ssDNA and dsDNA, thus the electrochemical response current is reduced leading to target detection. This is because the charge density of G-quadruplex/DNA is twice as high as that of unfolded ssDNA. Tang et al. (2012) reported construction of a sandwich electrochemical immunosensor by using hemin/G-quadruplex based DNAzyme concatemers as electrocatalyst and biolabels for the highly sensitive IgG1 detection. Wu et al. (2018) designed a highly sensitive thrombin sensor based on peptide enhanced hemin/G-quadruplex electrocatalysis and nanocomposite nanocarrier. G-quadruplex increases the resistance to nuclease, improves the electrochemical activity, and further amplifies the signal with nanocomposites. G-quadruplex electrochemical DNA sensors are therefore a promising area of future research. The electrochemical induction system can be used to detect thrombin. The sensors modified by G-quadruplex functional molecules can effectively screen the electroactive molecules and amplify the signal. The detection substance associated with nucleic acid causes the destruction or formation of G-quadruplex thus leading to the target detection. The application of G-quadruplex in biosensors improves the sensitivity, affinity and specificity of target detection (Tucker et al., 2012; Ying et al., 2003).

Terminal transferase (TDT) is a template free DNA polymerase that can recognize the end of DNA3′-OH. G-quadruplex/hemin DNAzyme can act as the nicotinamide adenine dinucleotide (NADH) oxidase and horseradish peroxidase (HRP)-mimicking enzyme (Qing et al., 2018). Liu et al. (2017) reported TDT-mediated formation of G-quadruplex/hemin DNAzyme for the development of a DNA-based electrochemical biosensor, which was successfully applied for the detection of alkaline phosphatase activity. With TDT as electronic medium, heme/G-quadruplex DNAzyme nanowires as HRP analog DNAzyme, further catalyzing reduction of H_2O_2, thus enhancing the electrochemical response signal.

3.1.2. Electrochemical G-quadruplex RNA biosensor

Besides DNA based G-quadruplex electrochemical sensors, RNA based G-quadruplex electrochemical sensors have been also intensively studied. The principle is similar to DNA based electrochemical G-quadruplex sensors (Lago et al., 2017). G-quadruplex based biosensors are used to detect miRNA. Chang et al. (2019) proposed a potential resolved dual signal homogeneous electrochemical strategy based on target initiation signal amplification ratio to detect target miRNA. Hairpin DNA/ssDNA/dsDNA labeled with electroactive dye was modified on indium tin oxide (ITO) electrode for accurate and effective target miRNA detection. Hou et al. (2015) reported a simple, sensitive and selective homogeneous electrochemical biosensor based on hybrid chain reaction (HCR) for the detection of miRNA. Tang et al. (2020) designed a G-quadruplex/rolling circle amplification (RCA) strategy in the presence

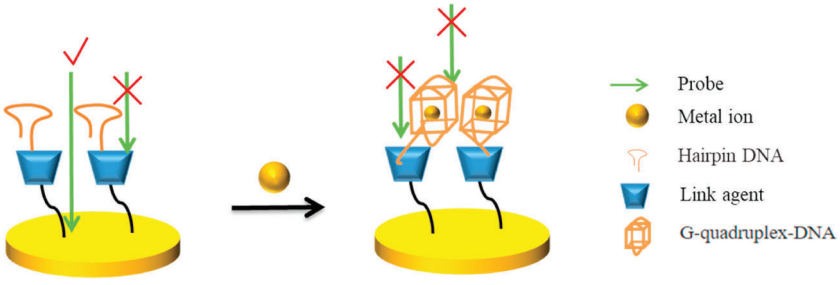

Fig. 4. Schematic diagram of G-quadruplex based biosensor for metal ions detection. In the presence of metal ions, the nucleic acid structure changes, leading to the modifications of contact area or distance between the probe molecule and the electrode. These modifications are then converted to the electrical signal changes for metal ions detection.

of exosomal miRNA-21, which is triggered by a chain shift, to be used in the highly specific and sensitive electrochemical sensing of exosomal miRNA (Fig. 5). The detection limit of electrochemical sensor was reduced to 2.75 fM for early diagnosis of cancer. Some studies have shown that 2 ′-fluoro modified RNA can detect vitamin B_{12} and methylcobalamin, with affinity constant (K_d) of 90 nM, with high biocompatibility and sensitivity. RNA G-quadruplex can interact with other nucleic acids to identify targets and amplify signals. By technical means, the signal is indirectly amplified to improve the sensitivity of nucleic acid for trace detection (Matsishin et al., 2017). It includes enzyme assisted target round (EATR) signal amplification and enzyme-free amplification. Zhou et al. (2020) prepared ultra-sensitive electrochemical biosensor of microRNA-141 (miRNA-141) by double amplification strategy. Through the click chemistry mediated self-assembly of nucleic acid chain, the two cleavage sequences containing G-quadruplex were connected, and the complementary G-quadruplex and miRNA-141 formed DNA-RNA hybrid duplex for specific recognition. The double amplification sensing system shows good miRNA-141 detection in the range of 0.1 pM–100 nM with the detection limit of 7.78 fM. It has high sensitivity and analytical performance and excellent resolution. Although RNA can be used as a recognition element for detection and signal amplification, its limitations include rapid degradation by nucleases in blood (Zhang et al., 2019; Arora et al., 2008). To solve this problem and to improve the performance of the biosensor, nucleic acid can be chemically modified.

3.2. Optical G-quadruplex biosensor

3.2.1. Fluorescent G-quadruplex biosensor

Besides G-quadruplex based electrochemical biosensor, a reliable and efficient G-quadruplex based fluorescent biosensor is also being developed. Guanine in G-quadruplex has lower oxidation, which can be used as the electron donor of a variety of fluorescence groups. After receiving electrons, the fluorescence group in the excited state generates fluorescence signals, and the fluorescence resonance transfer occurs in a variety of dyes (Ying et al., 2003; Wu et al., 2018). Organic fluorescent groups including crystal violet (CV) (Kong et al., 2009), thiazole orange (TO) (Lubitz et al., 2010), protoporphyrin IX (PPPIX) (Zhang et al., 2012), thioflavin T (ThT) (Mohanty et al., 2013) and their analogues (Kataoka et al., 2014), metal complexes such as Pt (II), IR (III) and Ru (II) complexes (Wang et al., 2015b), aggregation induced emission (AIE) substances (Li et al., 2018), and other groups with fluorescence properties are used as fluorescence signals for G-quadruplex biosensor. For example, the fluorescence signal of NMM itself is very weak, but can produce strong fluorescence after binding to G-quadruplex (Kreig et al., 2015; Yang et al., 2017). TO was shown to be a good G-quadruplex selective fluorescent probe for the design of novel nucleic acid biosensor (Lu et al., 2015). The fluorescence probe combines with G-quadruplex, and the addition of the target compound leads to the change of fluorescence signal intensity for accurate and sensitive target detection. The G-quadruplex based fluorescent DNA sensor is used to detect glucose (Bo et al., 2013), ATP (Kong et al., 2010b), nucleic acid molecules (Nakayama and Sintim, 2009) and other substances. It uses fluorescence free labeling and the principle of fluorescence resonance energy transfer to amplify the signal and to reduce the detection limit. Qiu et al. (2017) designed CdTe/CdSe quantum dots and hemin/G-quadruplex DNAzyme fluorescent biosensor for rolling cycle amplification and chain hybridization sensitive detection of lysozyme. In this biosensor, the fluorescence signal decreased with the increasing concentration of lysozyme. Fluorescence G-quadruplex sensor has also an application in the detection of H_2O_2. Besides detecting H_2O_2, H_2O_2 can also been used in the G-quadruplex/hemin DNAzyme for the fluorescent detection of DNA, aptamer–thrombin complexes, and probing the activity of glucose oxidase (Golub et al., 2011). In addition, G-quadruplex/hemin DNAzyme combined signal amplifier was also used to detect other biomolecules.

3.2.2. Colorimetry G-quadruplex biosensor

In colorimetry G-quadruplex biosensors, G-quadruplex is combined with metal nanoparticles or ABTS and the color changes lead to the target detection. G-quadruplex combines with hemin to form DNAzyme with similar catalytic properties of HRP. In the structure of G-quadruplex/hemin complex, the redox reaction between hydrogen and ABTS lead to the color change and the target molecule detection. Li et al. (2012) developed a bioluminescence sensor for cholesterol detection by using the peroxidase function of G-quadruplex structure. With the help of G-quadruplex structure, H_2O_2 oxidizes the achromatic $ABTS^{2-}$ and generates green $ABTS^{-}$ using cholesterol oxidation to generate H_2O_2. Cholesterol is detected due to the correlation of the intensity of the color signal with the amount of cholesterol. (Nie et al., 2015). Cagnin et al. (2009) constructed a biosensor to detect ExoIII by using the specific function of ExoIII 3′ → 5′ DNA double strand, combined with the structure of G-quadruplex. Without ExoIII, no signal was produced as the G-quadruplex/DNA sequence was covered by its complementary chain and unable to form G-quadruplex. However, after addition of ExoIII, G-quadruplex forms spontaneously to generate signals for ExoIII detection. Wang et al. (2015a,b) developed a G-quadruplex/hemin DNAzyme biosensor for nuclease S1 detection by combining the ability of nuclease S1 to cut DNA or RNA single strand with high specificity.

3.3. Other G-quadruplex biosensors

G-quadruplex biosensors combining photochemical and electrochemical methods, called photoelectrochemical (PEC) biosensors have been also engineered. The change of photocurrent is caused by the recognition of analyte. These biosensors attract research interest due to the low background signal, easy miniaturization and low cost. The choice of the material of photocathode in PEC sensor was shown to be of

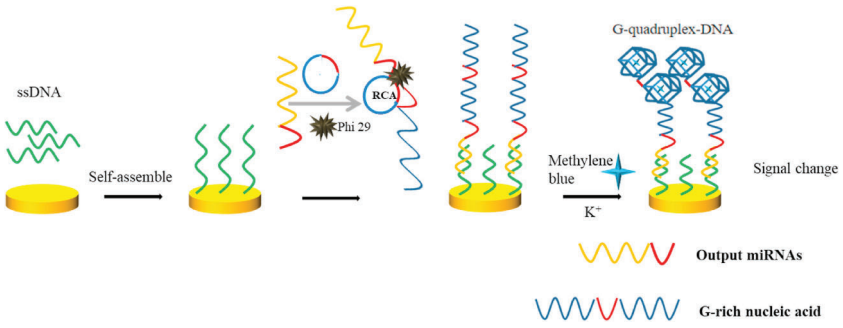

Fig. 5. Schematic illustration of exosome G-quadruplex electrochemical RNA biosensor. One end of miRNAs produces a large number of G-rich sequences through DNA polymerase, while the other end hybridizes with ssDNA to anchor rolling circle amplification (RCA) products on the electrode. The RCA products are incubated with K^+ and MB, and the signal indicator MB is embedded into the G-quadruplex structure to generate a measurable electrochemical signal (Tang et al., 2020).

particular importance. Lv et al. (2017) developed a novel photoelectrochemical sensor with *p*-$CuBi_2O_4$ semiconductors for disease-related proteins detection by using hemin/G-quadruplex DNAzyme on gold nanoparticles. Zhang et al. (2018b) designed a photoelectrochemical biosensor using CdS:Mn quantum dot-functionalized g-C3N4 nanohybrids as signal-generation tags, and DNAzyme as biocatalysts to detect prostate specific antigen. In addition, other biosensors based on G-quadruplex have also been studied, such as surface plasmon resonance (SPR) G-quadruplex biosensor (Pelossof et al., 2011). In this study, G-quadruplex/hemin and Au nanoparticles (NPs) were used as cooperative labels for amplified DNA sensing, aptasensing, and detection of Hg^{2+} ions. G-quadruplex/hemin-stimulated dielectric changes on the surface, as a result of recognition events, providing a readout signal for the SPR.

4. Virus detection by G-quadruplex biosensor

4.1. Common virus detection by G-quadruplex biosensor

As G-quadruplex sequences have been identified in a number of viruses; they are promising targets of novel antiviral drugs (Feng et al., 2014). Furthermore, G-quadruplex structure has been shown to have an impact on the whole life cycle of virus, including replication, recombination and gene expression control. G-quadruplex can be therefore used for detecting and inhibiting a whole range of viruses, such as hepatitis A virus (HAV) (Ma et al., 2017), Epstein-Barr virus (EBV) (Platella et al., 2017), cauliflower mosaic virus (CaMV) (Ruggiero and Richter, 2018), SARS-CoV (Tan et al., 2009) and simian virus 40 (SV40) (Lago et al., 2017). The versatility and plasticity of the G-quadruplex forming sequences allow them to be used in different types of detection tests. Several sensing strategies have been developed and combined with various sensors, such as quartz crystal microbalance (QCM), surface plasmon resonance (SPR), fluorescence, colorimetry, electrophoresis, electrochemistry, electrochemiluminescence (ECL) and field effect transistor (Ma et al., 2017; Platella et al., 2017; Ruggiero and Richter, 2018; Tan et al., 2009).

4.2. SARS-CoV-2 detection by G-quadruplex biosensor

Coronaviruses, such as SARS-CoV and Middle East Respiratory Syndrome Coronavirus (MERS-CoV) have caused severe epidemics in the past decades; however, the currently ongoing pandemic caused by the novel coronavirus SARS-CoV-2 has already surpassed them by far by the number of the infected people and the economic damage (Narayanan et al., 2003). The systematic analysis shows that SARS-CoV-2 and SARS-CoV are more closely related to each other than to MERS-CoV (Ji et al., 2020). Both, SARS-CoV and SARS-CoV-2, are enveloped coronaviruses with a single strand RNA genome approximately 30 KB long. Nonstructural protein 3 (NSP3) of SARS-CoV is a component of viral replicase complex, which contains a domain called SARS unique domain (SUD) interacting with G-quadruplex. G-quadruplex in coronaviruses can participate in their replication and escape from the host's immune system (Métifiot et al., 2014). A G-quadruplex-binding domain within SUD was shown to be indispensable for the activity of the SARS-CoV replication-transcription complex (Kusov et al., 2015). Since 2019, there have been large outbreaks of COVID-19 disease caused by SARS-CoV-2 in various countries with significant global impact (Di Giambenedetto et al., 2020). During infection, the envelope of SARS-CoV-2 is fused with the membrane of human mucosal cells, which leads to the release of the viral genetic material into the host cell and its replication. SARS-CoV-2 then spread further to the trachea, bronchi and alveoli causing pneumonia. The main symptoms of COVID-19 patients are fever, dry cough, fatigue, shortness of breath and dyspnea (Zhou et al., 2020). SARS-CoV-2 is highly contagious and can even cause death of the infected patients. Moreover, the asymptomatic carriers of SARS-CoV-2 are also a potential risk (Di Giambenedetto et al., 2020). At present, no effective vaccine is available for the treatment of COVID-19 (Li, 2020). Therefore, rapid and reliable detection of SARS-CoV-2, timely isolation of the virus carriers, blocking the spread of the virus and taking corresponding countermeasures are the key to combat COVID-19 pandemic (Walls, 2020).

Spike (S) protein, matrix (M) protein, envelope (E) protein and nucleocapsid (N) on the surface of SARS-CoV-2 are the most obvious potential targets for detection and treatment of COVID-19. Angiotensin converting enzyme II (ACE2) is the receptor of SARS-CoV-2 on the surface of the host cells to which SARS-CoV-2 S protein binds with high affinity (Wang et al., 2020).

Currently used SARS-CoV-2 detection methods include nucleic acid and serological detection. Real time reverse transcriptase polymerase chain reaction (RT-PCR) based on nucleic acid detection has been widely used as the gold standard diagnostic method for SARS-CoV-2 identification. Consequently, commercial RT-PCR kits are frequently used to detect SARS-CoV-2. Furthermore, the traditional RT-PCR detection method was improved to increase its scale, speed and ease of use. Roni et al. (2020) implemented large-scale ensemble RNA extraction and RT-PCR for an efficient high-throughput detection SARS-CoV-2. The conventional RT-PCR method for SARS-CoV-2 detection requiring RNA extraction step is time-consuming. To address this issue, Merindol et al. (2020) developed an improved RT-PCR based method for direct SARS-CoV-2 detection, which does not require RNA extraction step and is therefore significantly faster. Another recently developed RT-PCR based method of SARS-CoV-2 detection is reverse transcription loop-mediated isothermal amplification (RT-LAMP) (Mei et al., 2020). Furthermore, a colorimetric detection assay was adapted to RT-LAMP method to increase its throughput.

Work over the last months led also to the development of improved methods for serological SARS-CoV-2 detection. Notably, serological detection of SARS-CoV-2 antibodies takes less time than nucleic acid detection. Zeng et al. (2020) developed a combined IgG-IgM immunochromatographic method for rapid, hypersensitive and highly specific detection of SARS-CoV-2 labeled with gold nanoparticles. The combination of IgM and IgG antibody immunoassay can be used as an important auxiliary diagnostic method of patients infected with SARS-CoV-2.

SARS-CoV-2 detection using biosensors is an exciting new area of research. Seo et al., 2020 reported engineering of a biosensor based on field effect transistor (FET) for detecting SARS-CoV-2 in clinical samples. The sensor is produced by coating specific antibody against S protein of SARS-CoV-2 on graphene sheet of FET. This device uses a highly sensitive COVID-19 immunodiagnostic method which does not require sample pretreatment or labeling.

Targeting G-quadruplex structures appears to be a promising alternative method for SARS-CoV-2 detection (Zhang et al., 2020). Credle et al. (2020) showed that based on aptamer probe ligation test, SARS-CoV-2 can be detected and its genotype can be effectively determined. This method is simple and does not require the nucleic acid extraction step.

Recently, we have identified 25 putative G-quadruplex-forming sequences (PQSs) in the genome of SARS-CoV-2 (Ji et al., 2020). The identified PQSs are located in the open reading frames of ORF1ab, spike (S), ORF3a, membrane (M) and nucleocapsid (N) genes of SARS-CoV-2. The PQSs located in S and N genes are of particular interest. S protein binds to the ACE2 receptor on the surface of the host cells and plays an important role in internalization of the virus into the host cell (Zhou et al., 2020). Based on SARS-CoV research, N protein of SARS-CoV-2 can be involved in the transcription, replication and RNA packaging (Narayanan et al., 2003).

The top-ranked PQSs (13385/PQS: 5′-GGUAUGUGGAAAGGUUAUGG-3′ and 24268/PQS: 5′-GGCUUAUAGGUUUAAUGGUAUUGG-3′) identified in our study were shown to form RNA G-quadruplex structures *in vitro* by multiple spectroscopic assays. Furthermore, microscale thermophoresis revealed a direct interaction of

the SARS-CoV-2 G-quadruplex structures with viral helicase (nsp13). Molecular docking modelling suggests that nsp13 distorts the G-quadruplex structure by allowing the guanine bases to be flipped away from the guanine quartet planes, thus facilitating their unfolding (Ji et al., 2020).

Some of the identified SARS-CoV-2 PQSs are well conserved in a wide range of other members of the Coronaviridae, while two top-ranked PQSs were strongly conserved only in the narrow range of Coronaviruses (Ji et al., 2020). Besides serving as potential targets for antiviral treatment against SARS-CoV-2, RNA G-quadruplex sequences identified in SARS-CoV-2 could be also used in the biosensors for the detection of viral helicase protein nsp13 of SARS-CoV-2.

5. Development prospect of G-quadruplex biosensor

G-quadruplex structures have a number of features suitable for novel biosensors. These include thermodynamic and chemical stability, non-immunogenicity, high specificity of interaction with the target, ease of manufacturing and storage, and the unique folding properties leading to different conformations, which can recognize specific targets, including proteins (Kolesnikova et al., 2019), viruses (Perrone et al., 2016) and bacteria (Roxo et al., 2019). Consequently, a large number of G-quadruplex have been developed and applied in treatment, administration and diagnosis. G-quadruplex can be directly used as therapeutic drugs, including anticoagulants (Avino et al., 2012), anticancer and antiviral agents (Dailey et al., 2010; Perrone et al., 2016). Most of the developed G-quadruplex have not been applied in biosensors yet and particularly the number of the engineered electrochemical G-quadruplex biosensors is low. However, we believe that G-quadruplex structures have a great potential to be used in biosensors.

AS1411 is one of the G-rich DNA nucleic acids in clinical trials for cancer treatment. Under certain conditions, it forms an antiparallel G-quadruplex structure with intramolecular interaction mode, which has high thermodynamic and chemical stability, and resistance to nuclease degradation (Yoon et al., 2010). AS1411 has been used in biosensors to efficiently and specifically detect Cu^{2+} (Soundararajan et al., 2009). In the fluorescent biosensor, the combination of AS1411 and Cu^{2+} hinders the hybridization between AS1411 and the complex, and the combination of AS1411 with the complementary chain without Cu^{2+} leads to the weakening of fluorescence signal and the highly sensitive detection of Cu^{2+}. Based on the specificity of AS1411 biomolecule binding, this can be used to detect cancer cell markers according to the signal changes resulting from G-quadruplex reaction or structural change after binding. Modified and applied in biosensor, it can generate electrical, optical and other signals for the highly sensitive and selective detection. Other G-rich AS1411 nucleic acid analogues developed for anticancer therapy can also be used in biosensors for detecting biomolecules, chemical molecules, ions and enzymes (Pedersen et al., 2011).

Series of G-quadruplex sequences have been derived for different targets, such as anticoagulant thrombin binding aptamer (TBA) (Phillips et al., 2009), antiviral agent G-quadruplex aptamer (ISIS5320) (Rajendran et al., 2013), G-quadruplex aptamer targeting ATP (Srinivasan et al., 2019), and HIV-1 G-quadruplex aptamers (Rajendran et al., 2013). Moreover, multiple G-quadruplex sequences were developed for a target, which share sequence similarity. Many of these G-quadruplex sequences were still not incorporated into biosensors. Compared to other biosensors, G-quadruplex biosensor has a number of advantages, such as high affinity, stability and easy regeneration (Johnson et al., 2008). The three-dimensional folding ability of G-quadruplex after combining with the target allows simple and direct detection (Srinivasan et al., 2019).

6. Summary and conclusions

In this review, we showed that the unique folding properties of G-quadruplex enable to recognize a wide range of targets, including proteins, viruses and bacteria. Compared with monoclonal antibodies, G-quadruplex structures have a number of advantages, such as simple scaffold, smaller volume, no immunogenicity, and reversibility of action. Furthermore, they are easy to manufacture and store. G-quadruplex structures are powerful alternatives to antibodies in targeted therapy, *in vitro* and *in vivo* diagnostics and biomarker testing. In a biosensor, G-quadruplex is used for the signal conversion and detection is achieved by DNA structure modification when G-quadruplex combines with the tested object. Furthermore, G-quadruplex can be combined with the adapter for specific target recognition and the signal can be amplified to improve the sensitivity and reduce the detection limit.

G-quadruplex structure has an impact on the whole life cycle of viruses, including replication, recombination and gene expression. G-quadruplex based biosensors can be therefore used for the detection of a broad spectrum of viruses. G-quadruplex structures have been recently identified in SARS-CoV-2 genome and besides serving as targets of antiviral drugs, they can be used in biosensors for SARS-CoV-2 detection.

7. Future perspectives

Compared with the traditional probes, G-quadruplex has a number of advantages, including smaller size, simpler synthesis and easier modification. Signal amplification can further improve sensitivity and detection limit of the biosensor. Although G-quadruplex biosensor has many advantages, some obstacles still remain: (I) The preparation and screening of suitable G-quadruplex molecules as probes. (II) The biological complexity of samples. (III) The further improvement of sensitivity and selectivity of G-quadruplex. In the future research, (I) The application of G-quadruplex in electrochemical sensor should be studied in detail as G-quadruplex structure modifications can generate different electrical signal levels for detection of specific targets. (II) The affinity of G-quadruplex to specific targets should be explored to generate stronger signals. (III) New methods to avoid G-quadruplex degradation by nucleases should be explored. (IV) Biosensors should be developed where G-quadruplex can be used as both the conversion and the recognition element. (V) G-quadruplex based biosensors with improved characteristics, such as low cost, simple operation, miniaturization and higher affinity, specificity and sensitivity should be developed.

Currently, COVID-19 still remains a global threat. Development of the G-quadruplex based biosensor for the fast and efficient SARS-CoV-2 detection is therefore of a great importance. The surface protein of SARS-CoV-2, potential target for the detection and treatment of this virus, can be recognized by the unique spatial structure of G-quadruplex. The selected G-quadruplex sequences, as recognition elements, can be combined with other signal molecules to engineer different types of biosensors, where SARS-CoV-2 is detected by reading electrochemical, florescent or colorimetry signal changes. G-quadruplex based biosensors have the potential to replace the antibody-based detection and to improve the diagnosis of SARS-CoV-2 and other pathogens.

CRediT authorship contribution statement

Hui Xi: Writing - original draft, Visualization, Writing - review & editing. **Mario Juhas:** Writing - review & editing. **Yang Zhang:** Conceptualization, Supervision, Visualization, Writing - review & editing.

Declaration of competing interest

The authors declare that they have no known competing financial interests or personal relationships that could have appeared to influence the work reported in this paper.

Acknowledgements

The work was supported by the Shenzhen Science and Technology Innovation Commission (Shenzhen Basic Research Project No. JCYJ20180306172131515).

References

Arora, A., Dutkiewicz, M., Scaria, V., Hariharan, M., Maiti, S., Kurreck, J., 2008. RNA 14, 1290–1296.
Avino, A., Fabrega, C., Tintore, M., Eritja, R., 2012. Curr. Pharm. Des. 18, 2036–2047.
Bielskutė, S., Plavec, J., Podbevšek, P., 2019. JACS 141, 2594–2603.
Biffi, G., Tannahill, D., McCafferty, J., Balasubramanian, S., 2013. Nat. Chem. 3, 182–186.
Bhattacharjee, S., Chakraborty, S., Sengupta, P.K., Bhowmik, S., 2016. J. Phys. Chem. B 120, 8942–8952.
Bo, H., Wang, C., Gao, Q., Qi, H., Zhang, C., 2013. Talanta 108, 131–135.
Burge, S., Parkinson, G.N., Hazel, P., Todd, A.K., Neidle, S., 2006. Nucleic Acids Res. 34, 5402–5415.
Cagnin, S., Caraballo, M., Guiducci, C., Martini, P., Ross, M., SantaAna, M., Lanfranchi, G., 2009. Sensors 9, 3122–3148.
Chang, J., Li, H., Li, F., 2019. Chem. Commun. 55, 10603.
Chen, X.C., Chen, B.S., Dai, J., Yuan, J.H., 2018. Angew. Chem. Int. Ed. 57, 4702–4706.
Chen, N., et al., 2020. Lancet 395, 507–513.
Chen, M., Hou, C., Huo, D., Yang, M., Fa, H., 2016. Appl. Surf. Sci. 364, 703–709.
Cheng, N., Shang, Y., Xu, Y., Zhang, L., Luo, Y., Huang, K., Xu, W., 2017. Biosens. Bioelectron. 91, 408–416.
Credle, J.J., Robinson, M.L., Gunn, J., Monaco1, D., Sie, B., Tchir, A., 2020. BioRxiv.
Dai, J., Carver, M., Punchihewa, C., Jones, R., Yang, D., 2007. Nucleic Acids Res. 35, 4927–4940.
Dailey, M.M., Clarke Miller, M., Bates, P.J., Lane, A.N., Trent, J.O., 2010. Nucleic Acids Res. 38, 4877–4888.
Debnath, M., Chakraborty, S., Kumar, Y.P., Chaudhuri, R., Jana, B., Dash, J., 2020. Nat. Commun. 11.
Deng, H., Sun, M., Wei, X.P., Li, H.Z., 2016. Chinese J. Anal. Chem. 44, 888–892.
Di Antonio, M., Ponjavic, A., Radzevičius, A., 2020. Nat. Chem. 56.
Di Giambenedetto, S., Ciccullo, A., Posteraro, B., Lombardi, F., Borghetti, A., Sanguinetti, M., 2020. Clin. Infect. Dis.
Fedeles, B.I., 2017. Proc. Natl. Acad. Sci. 114, 2788–2790.
Feng, C., Dai, S., Wang, L., 2014. Biosens. Bioelectron. 59, 64–74.
Frank-Kamenetskii, M.D., Mirkin, S.M., 1995. Annu. Rev. Biochem. 64, 65–95.
Fujii, A., Nakagawa, O., Kishimoto, Y., Nakatsuji, Y., Nozaki, N., Obika, S., 2019. ChemBioChem 21, 860–864.
Gargallo, R., 2014. Anal. Biochem. 466, 4–15.
Gao, A., Wang, Y., He, X., Yin, X., 2012. Chin. J. Anal. Chem. 40, 1471–1476.
Gatto, B., Palumbo, M., Sissi, C., 2009. Curr. Med. Chem. 16, 1248–1265.
Ge, Z., Lin, M., Wang, P., Pei, H., Yan, J., Shi, J., Zuo, X., 2014. Anal. Chem. 86, 2124–2130.
Gibriel, A.A., Adel, O., 2017. Mutat. Res-Rev. Mutat. 773, 66–90.
Golub, E., Freeman, R., Niazov, A., Willner, I., 2011. The Analyst 136, 4397.
Gowan, S.M., 2002. Mol. Pharmacol. 61, 1154–1162.
Guo, L., Nie, D., Qiu, C., Zheng, Q., Wu, H., Ye, P., Chen, G., 2012. Biosens. Bioelectron. 35, 123–127.
Hou, T., Li, W., Liu, X., Li, F., 2015. Anal. Chem. 87, 11368–11374.
Huang, R., He, L., Xia, Y., 2019. Small 15, 1900735.
Ji, D.Y., Juhas, M., Tsang, C.M., Kwok, C.K., Li, Y., Zhang, Y., 2020. bbaa11400 1–11.
Johnson, J., Smith, J., Kozak, M., Johnson, F., 2008. Biochimie 90, 1250–1263.
Kataoka, Y., Fujita, H., Kasahara, Y., Yoshihara, T., Tobita, S., Kuwahara, M., 2014. Anal. Chem. 86, 12078–12084.
Kolesnikova, S., Srb, P., Vrzal, L., Lawrence, M.S., Veverka, V., Curtis, E.A., 2019. ACS Chem. Biol. 14, 1951–1963.
Kong, D.M., Guo, J.H., Yang, W., Ma, Y.E., Shen, H.X., 2009. Biosens. Bioelectron. 25, 88–93.
Kong, D.M., Xu, J., Shen, H.X., 2010a. Anal. Chem. 82, 6148–6153.
Kong, D.M., Yang, W., Wu, J., Li, C.X., Shen, H.X., 2010b. Analyst 135, 321–326.
Kreig, A., Calvert, J., Sanoica, J., Cullum, E., Tipanna, R., Myong, S., 2015. Nucleic Acids Res. 43, 7961–7970.
Kuauert, M.P., 2001. Hum. Mol. Genet. 10, 2243–2251.
Kusov, Y., Tan, J., Alvarez, E., Enjuanes, L., Hilgenfeld, R., 2015. Virology 484, 313–322.
Lago, S., Tosoni, E., Nadai, M., Palumbo, M., Richter, S.N., 2017. BBA - Gen Subjects 1861, 1371–1381.
Laguerre, A., Hukezalie, K., Winckler, P., Katranji, F., Chanteloup, G., Pirrotta, M., Monchaud, D., 2015. J. Am. Chem. Soc. 137, 8521–8525.
Li, H., Chang, J., Gai, P., Li, F., 2018. ACS Appl. Mater. Int. 10, 4561–4568.
Li, R., Xiong, C., Xiao, Z., Ling, L., 2012. Anal. Chim. Acta 724, 80–85.
Li, L., 2020. Lancet. Resp. Med. 8.
Liang, Y., Zhang, Z., Wei, H., Hu, Q., Deng, J., Guo, D., Cui, Z., Zhang, X., 2011. Biosens. Bioelectron. 28, 270–276.
Liu, Y., Lai, P., Wang, J., Xing, X. wen, Xu, L., 2020. Chem. Commun. 56.
Liu, S., Wei, M., Wang, X., Shi, C., Kuang, S., Ma, C., 2019. Talanta 120628.
Liu, X., Freeman, R., Golub, E., Willner, I., 2011. ACS Nano 5, 7648–7655.
Liu, Y., Xiong, E., Li, X., Li, J., Zhang, X., Chen, J., 2017. Biosens. Bioelectron. 87, 970–975.
Lou, X., Leung, C., Dong, C., Hong, Y., Chen, S., Zhao, E., Tang, B., 2014. RSC Adv. 4, 33307–33311.
Lu, Y.J., Deng, Q., Hu, D.P., Wang, Z.Y., Huang, B.H., Du, Z.Y., Chow, C.F., 2015. Chem. Comm. 51, 15241.
Lubitz, I., Zikich, D., Kotlyar, A., 2010. Biochemistry 49, 3567–3574.
Lv, S., Zhang, K., Lin, Z., Tang, D., 2017. Biosens. Bioelectron. 96, 317–323.
Ma, D.L., Wu, C., Dong, Z.Z., Tam, W.S., Wong, S.W., Yang, C., Leung, C.H., 2017. Chem. Asian J. 12, 1851–1860.
Margulies, D., Hamilton, A.D., 2009. Angew. Chem. Internat. Ed. 48, 1771–1774.
Matsishin, M., Rachkov, A., Lopatynskyi, A., Chegel, V., Soldatkin, A., El'skaya, A., 2017. Nanoscale Res. Lett. 12, 252.
Mei, F., Bonifazi, M., Menzo, S., Sedizari, M., Paolini, L., Gasparini, S., 2020. Chest.
Merindol, N., Pépin, G., Marchand, C., Rheault, M., Peterson, C., Poirier, A., Danylo, A., 2020. J. Clin. Virol. 128, 104423.
Métifiot, M., Amrane, S., Litvak, S., Andreola, M.L., 2014. Nucleic Acids Res. 42, 12352–12366.
Mohanty, J., Barooah, N., Dhamodharan, V., Harikrishna, S., Pradeepkumar, P.I., Bhasikuttan, A.C., 2013. J. Am. Chem. Soc. 135, 367–376.
Murat, P., Balasubramanian, S., 2014. Curr. Opin. Genet. Dev. 25, 22–29.
Nakayama, S., Sintim, H.O., 2009. JACS 131, 10320–10333.
Narayanan, K., Kim, K.H., Makino, S., 2003. Virus Res. 98, 131–140.
Nie, W., Gupta, G., Crone, B.K., Liu, F., Smith, D.L., Ruden, P.P., Mohite, A.D., 2015. Adv. Sci. 2, 1500024.
Olsen, C.M., Marky, L.A., 2009. Methods Mol. Biol. 147–158.
Pedersen, E.B., Nielsen, J.T., Nielsen, C., Filichev, V.V., 2011. Nucleic Acids Res. 39, 2470–2481.
Pelossof, G., Tel-Vered, R., Liu, X.Q., Willner, I., 2011. Chem. Eur. J. 17, 8904–8912.
Peng, Y., Wang, X., Xiao, Y., Feng, L., Zhao, C., Ren, J., Qu, X., 2009. J. Am. Chem. Soc. 131, 13813–13818.
Perrone, R., Butovskaya, E., Lago, S., Garzino-Demo, A., Pannecouque, C., Palù, G., 2016. Int. J. Antimicrob. Agents 47, 311–316.
Phan, A.T., 2002. Nucleic Acids Res. 30, 4618–4625.
Phillips, J.A., Xu, Y., Xia, Z., Fan, Z.H., Tan, W., 2009. Anal. Chem. 81, 1033–1039.
Phillips, K., Dauter, Z., Murchie, A.I.H., Lilley, D.M.J., Luisi, B., 1997. J. Mol. Biol. 273, 171–182.
Platella, C., Riccardi, C., Montesarchio, D., Roviello, G.N., Musumeci, D., 2017. BBA - Gen Subjects 1861, 1429–1447.
Qing, M., Yuan, Y., Cai, W., Xie, S., Tang, Y., Yuan, R., Zhang, J., 2018. Sens. Actuat. B-Chem. 263, 469–475.
Qiu, Z., Shu, J., He, Y., Lin, Z., Zhang, K., Lv, S., Tang, D., 2017. Biosens. Bioelectron. 87, 145–162.
Raguseo, F., Chowdhury, S., Minard, A., Di Antonio, M., 2020. Chem. Commun. 56.
Rajendran, A, Endo, M, Hidaka, K, Tran, P.L.T, Mergny, J.L, Gorelick, R.J, Sugiyama, H, 2013. JACS 135, 18575–18585.
Rhodes, D., Lipps, H.J., 2015. Nucleic Acids Res. 43, 8627–8637.
Roni, B.A., Agnes, K., Matan, S., Tal, S., 2020. Clin. Microbiol. Infect.
Roxo, C., Kotkowiak, W., Pasternak, A., 2019. Molecules 24, 3781–3792.
Ruggiero, E., Richter, S.N., 2018. Nucleic Acids Res. 46, 3270–3283.
Seo, G., Lee, G., Kim, M.J., Baek, S.-H., Choi, M., Ku, K.B., Kim, S.I., 2020. ACS Nano 14, 5135–5142.
Shi, L., Yu, Y.Y., Chen, Z.G., Zhang, L., He, S.J., Shi, Q.J., Yang, H.Z., 2015. RSC. Adv. 5, 11541.
Shivalingam, A., Izquierdo, M.A., Marois, A.L., Vyšniauskas, A., Suhling, K., Kuimova, M. K., Vilar, R., 2015. Nat. Commun. 6, 8178.
Smargiasso, N., Rosu, F., Hsia, W., Colson, P., Baker, E.S., Bowers, M.T., Gabelica, V., 2008. JACS 130, 10208–10216.
Soundararajan, S., Wang, L., Sridharan, V., Chen, W., Courtenay-Luck, N., Jones, D., Spicer, E.K., Fernandes, D.J., 2009. Mol. Pharmacol. 76, 984–991.
Srinivasan, S., Ranganathan, V., DeRosa, M.C., Murari, B.M., 2019. Anal. Bioanal. Chem. 411, 1319–1330.
Tan, J., Vonrhein, C., Smart, O.S., Bricogne, G., Bollati, M., Kusov, Y., Hilgenfeld, R., 2009. PLoS Pathog. 5, e1000428.
Tang, J., Hou, L., Tang, D., Zhang, B., Zhou, J., Chen, G., 2012. Chem. Comm. 48, 8180.
Tang, X., Wang, Y., Zhou, L., Zhang, W., Yang, S., 2020. Microchim. Acta 187, 172–178.
Tateishi-Karimata, H., Kawauchi, K., Sugimoto, N., 2018. JACS 140, 642–651.
Tauchi, T., Shinya, K., Sashida, G., Sumi, M., Okabe, S., Ohyashiki, J.H., Ohyashiki, K., 2006. Oncogene 25, 5719–5725.
Tuntiwechapikul, W., Taka, T., Béthencourt, M., Makonkawkeyoon, L., Randall Lee, T., 2006. Bioorg. Med. Chem. Lett 16, 4120–4126.
Tucker, O., Shum, W.T., Tanner, J., 2012. Curr. Pharm. Des. 18, 2014–2026.
Viglasky, V., Hianik, T., 2013. Phys. Biophys. 32, 149–172.
Wang, D., Zhao, W., Li, J., 2020. JAMA 292–298.
Walls, A.C., et al., 2020. Cell 181, 281–292.
Wang, M., Wang, W., Kang, T.S., Leung, C.H., Ma, D.L., 2015a. Anal. Chem. 88, 981–987.
Wang, M., Wang, W., Liu, C., Liu, J., Kang, T.-S., Leung, C.H., Ma, D.L., 2017. Mater. Chem. Front. 1, 128–131.
Wang, Z., Zhao, J., Bao, J., Dai, Z., 2015b. ACS. Appl. Mater. Int. 8, 827–833.
Wu, K., Ma, C., Deng, Z., Fang, N., Tang, Z., Zhu, X., Wang, K., 2018. Talanta 182, 142–147.
Wu, Y., Zou, L., Lei, S., Yu, Q., Ye, B., 2017. Biosens. Bioelectron. 97, 317–324.
Xu, M., Gao, Z., Wei, Q., Chen, G., Tang, D., 2015. Biosens. Bioelectron. 74, 1–7.
Yan, Y.Y., Tan, J.H., Lu, Y.J., Yan, S.C., Wong, K.Y., Li, D., Huang, Z.S., 2013. BBA 1830, 4935–4942.
Yang, H., Wu, Q., Su, D., Wang, Y., Li, L., Zhang, X., 2017. Anal. Sci. 33, 133–135.
Ying, L., Green, J.J., Li, H., Klenerman, D., Balasubramanian, S., 2003. Proc. Natl. Acad. Sci. 100, 14629–14634.

Yoon, V., Fridkis-Hareli, M., Munisamy, S., Lee, J., Anastasiades, D., Stevceva, L., 2010. Curr. Med. Chem. 17, 741–749.
Yu, P., Zhu, J., Zhang, Z., Han, Y., Huang, L., 2020. J. Infect. Dis. 221.
Yuan, Q., Liu, Y., Ye, C., Sun, H., Dai, D., Wei, Q., Lin, C.T., 2018. Biosens. Bioelectron. 111, 117–123.
Yuan, W., Wan, L., Peng, H., Zhong, Y., Cai, W., Zhang, Y., Wu, J., 2020. Cell Biochem. Funct. 1–9.
Zeng, l., Li, Y., Xu, C., 2020. Mater. Chem. Front.
Zeraati, M., Langley, D.B., Schofield, P., Moye, A.L., Rouet, R., Hughes, W.E., Christ, D., 2018. Nat. Chem. 10, 631–637.
Zhang, J., Harvey, S.E., Cheng, C., 2019. Nucleic Acids Res. 47, 3667–3679.
Zhang, R.X., Ke, X., Gu, Y., Liu, H.D., Sun, X., 2020. BioRxiv.
Zhang, Y., Lai, B., Juhas, M., 2019b. Molecules 24, 941.
Zhang, K., Lv, S., Lin, Z., Li, M., Tang, D., 2018. Biosens. Bioelectron. 95, 159–166.
Zhang, Z., Sharon, E., Freeman, R., Liu, X., Willner, I., 2012. Anal. Chem. 84, 4789–4797.
Zhang, S., Sun, H.X., Wang, L.X., Liu, Y., Chen, H.B., Li, Q., Guan, A.J., Liu, M.R., Tang, T.L., 2018b. Nucleic Acids Res. 46, 7522–7532.
Zhang, Y., Wang, L., Wang, Y., Dong, Y., 2018a. Sensors 18, 2179–2183.
Zhou, P., Yang, X.L., Wang, X.G., Hu, B., Zhang, L., Zhang, W., Shi, Z.L., 2020. Nature 579, 270–273.
Zhou, J., Yuan, G., 2007. Acta Chim. Sin. 16, 1728–1732.
Zou, L., Ruan, F., Huang, M., Liang, L., Huang, H., Hong, Z., Yu, J., Kang, M., Song, Y., Xia, J., Guo, Q., Song, T., He, J., Yen, H., Peiris, M., Wu, J., 2020. N. Engl. J. Med. 382, 1177–1179.